Energy Consumption of Control Schemes for the Pioneer 3DX Mobile Robot: Models and Evaluation

Lotfi Jaïem, Didier Crestani, Lionel Lapierre, Sébastien Druon

JrnlID 10846_ArtID 1374_Proof#1 - 14/04/2021

Journal of Intelligent & Robotic Systems _####################_
https://doi.org/10.1007/s10846-021-01374-6

REGULAR PAPER

Energy Consumption of Control Schemes for the Pioneer 3DX Mobile Robot: Models and Evaluation

Lotfi Jaiem[1] · Didier Crestani[1] · Lionel Lapierre[1] · Sébastien Druon[1]

Received: 8 January 2020 / Accepted: 23 March 2021

Abstract

Energy is a key feature that must be explicitly managed for long-term autonomous robotic missions. Many research studies have addressed the energy issue, developed energy-aware motion control or integrated energy in mission objectives. However, few studies have comprehensively assessed the impact of software and hardware choices on power consumption of robots. Based on experimental analysis and according to the selected control scheme and hardware configuration, this paper proposes energy consumption models for the Pioneer 3DX. The proposed models highlight the existence of an optimal velocity that minimizes motion energy. These models are experimentally evaluated and discussed.

Keywords Robot energy consumption · Laptop energy consumption · Energy model evaluation · P3DX robot

1 Introduction

Mobile robotics aims at addressing a large range of mission classes. Unlike industrial robotics, the available embedded energy is limited for autonomous robots. Each robot decision has a direct impact on its energy stock and consequently on its operational capability to perform long-term missions. Energy is hence a key issue with regard to autonomous mobile robotic missions. Many research studies have focused on minimizing energy consumption. However few studies have dealt with the prediction of the energy consumption for various mission tasks according to the software and hardware resources involved. The availability of such models is essential to be able to efficiently manage real autonomous robotic missions. The definition of such models is the main topic of this paper.

Energy is a pivotal issue in autonomous robotics [3]. Research on this topic can be roughly divided into three main complementary levels: component, robot system and mission levels.

The *component level* aims to reduce energy consumption using energy-aware hardware or software techniques using Dynamic Power Management (DPM) techniques [4]. At the *robot system level* the goal is to model the robot's energy consumption according to a considered robotic task and trajectory. Finally, the *mission level* intends to model the mission energy consumption, using robot system energy information, according to the mission plan.

The energy issue has been less addressed at the robot system level. It is a difficult issue and most of autonomous robotic studies usually neglect the energy problem. Some studies focus on energetic optimality of locomotion strategy (e.g. legged robots [30], or snake like systems [13]). Here we are not addressing this question since our goal is to tackle the global energetic consumption at the mission level. In that context, short-term mission generally considers that the system embeds sufficient amount of energy to realize the planned tasks. However, it becomes a key issue when long-term or hazardous missions are concerned.

The robot system level is needed crossing point to address the mission level. Previous studies mainly focused on the identification of robot energy consumption model along energy-aware trajectories, for missions involving only a unique control task. Mei in [19] conducted an experimental analysis of power consumption of a Pioneer 3DX mobile robot, considering the motion energy, the sensors, and the computer consumption. Several studies have focused on the determination of optimal velocity profiles minimizing energy consumption, along predefined

✉ Lionel Lapierre
lapierre@lirmm.fr

[1] Laboratoire d'Informatique Robotique et Microélectronique de Montpellier (LIRMM), UMR 5506, Université de Montpellier, C.N.R.S., 161 rue Ada, 34 095 Montpellier Cedex 5, Montpellier, France

trajectories. Kim and Kim in [14] focused on straight-line motion on flat surfaces. The same issue was addressed in Tokekar et al. [27, 28]. Different problems have been considered from a single segment to a path composed of N segments of straight lines and curves. Mei et al. in [31] explored different motion plan scenarios (scan lines, spiral square spirals) to cover an open area from an energy viewpoint to determine the most efficient one. Energy prediction approaches integrating rolling resistance for unmanned ground vehicles was addressed by Sadrpour et al. in [23] [24] and [25] using mission prior knowledge (road grade and rolling resistance information, driving style, etc.). These approaches were used in [9] to build an energy efficient coverage plan for ground robot, where simulation results were presented. Finally, in [21], an on-line prediction model for energy consumption of a Khepera III robot integrating the impact of the sensors was presented and experimentally evaluated on a very short mission.

Several experimental analyses of energy consumption have been published but this work aims to propose a generic formulation of the energy power consumption at the robot system level considering the different control schemes (CS) and their associated hardware and sotftware resources.The main contributions are the following:

- We are considering a predictive energy consumption model at the robot system level.
- We are considering here a multiple batteries system, one devoted to the platform, the other supplying the on-board laptop.
- This study enlights in detail the software impact of the algorithms selection on the energy consumption.
- A new model involving motion energy consumption, velocity and covered distance, for a straight line path is proposed for a Pioneer P3DX.
- Finally, most studies concerning energy consumption models evaluate them locally on rather short robot motion pathways. It is however essential to estimate their accuracy along longer and more complex missions. This accuracy must remain acceptable to be able to efficiently manage energy consumption at the mission level.

The paper is organized as follows. Section 2 presents first the hardware and software architectures and the experimental environment used. A general flowchart of the proposed method is provided and a generic formulation of the power consumption is exposed. In a first step, Section 3 builds the models proposed for the architecture components as part of the previous generic formulation, and compares them to previous studies. In a second step, the accuracy of the generic model is evaluated according to a simple forward motion or a more complex patrolling mission. Finally the last section draws general and specific conclusions about this study. It also shows that the proposed study can address the energy management at the mission level and exposes some on going works.

2 Experimental Context and Proposed Methodology

2.1 The Robotic Platform and the Control Architecture

Based on a classic Pioneer 3DX mobile robot, the robot platform (Fig. 1a) of 25 kg weight was equipped with many additional sensors and electronic devices to be able to implement different motion, location and image analysis control schemes, and to perform online energy monitoring.

The two top to tail URG-04 LX Hokuyo 240°lasers (LAS) allow 360° scanning of the surrounding environment. A camera (Kinect©) system (KIN) is used to perform image analysis. Two added switchboards with two command channels allow for independent connection or disconnection of the power supply of the two laser devices and the camera, according to the chosen control scheme. An embedded USB wattmeter (Yocto-Watt) was also integrated to perform online measurements of the energy delivered by the robot battery.

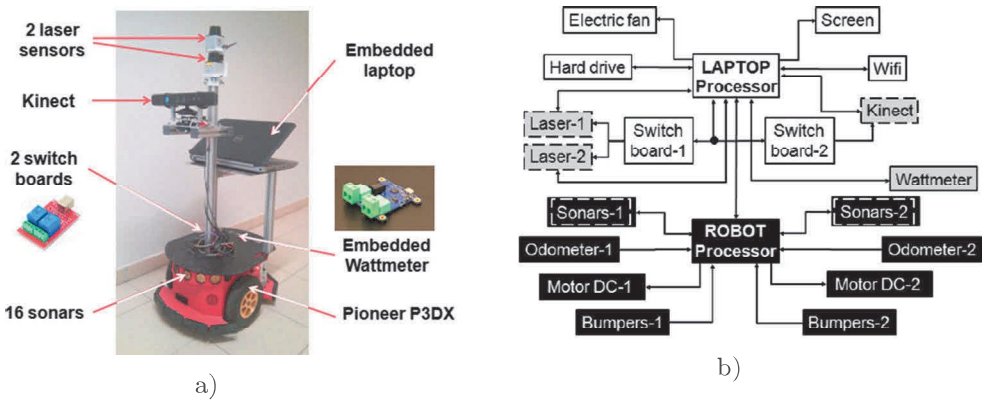

Fig. 1 The Pioneer P3DX. **a** The robotic platform. **b** The hardware architecture

The on-board laptop supports a Linux-RTAI operating system, running the control architecture according to the Real-Time middleware ConTract [22] managing the control scheme selection during autonomous robotic missions. Its battery supplies the laptop processor, screen, wifi board, hard drive and electric fan. It also supports USB communication with the lasers, Kinect, switchboards, wattmeter and the robot micro-controller. The laptop battery consumption is estimated using the Linux *uevent* system file of the battery state. This file allows for on-line monitoring of the battery current and voltage, and an estimation of the remaining laptop battery energy.

The hardware architecture of the robotic platform is presented in Fig. 1b. Elements supplied by the robot battery indicated with black boxes, while those supplied by the laptop battery are white boxes. Switchable components (switching on/off the electric supply) are shown with dotted lines. Furthermore, note that these components and the wattmeter are connected to the laptop using USB for data exchange, but are supplied by the robot battery (grey boxes).

A robotic mission can be divided into a set of potential overlapped areas where different robotic tasks (moving forward, communicating, locating, etc.) take place. A robotic task requires periodic call up of sensor information, control or processing algorithms gathered in a control scheme. The control architecture managed the following control schemes, which involves specific sensors and algorithms.:

- Simple path following (SPF) with obstacle avoidance (using 1, 2 lasers or sonars), as described in [18].
- Centring motion (CM), where the system uses proximity measurements to follow the central line of a corridor.
- Dead-reckoning navigation using odometers (ODO).
- Navigation using grid-based localization (GBL) using 2 top to tail lasers.
- QR-code navigation (QRCN), allowing the system to regularly control the estimation of its position using a camera.
- Image analysis (IA) performs a visual analysis of an image of a valve to obtain its status (open/close).

The hardware and software context of the study being presented, a generic formulation of the power consumption of a control scheme is now proposed (Table 1).

2.2 Power and Energy Consumption Models: Generic Formulation

In the following we adapt the formulation proposed in [21] for a Khepera robot. Generally the instantaneous power consumption P(CS) for a given CS can be divided into dynamic and static parts. The dynamic part P_{Dyn} denotes the *time-varying* power consumption. For example, motion power consumption depends on the chosen velocity and sonar power consumption depends on the chosen frequency rate. The static part P_{Stat} denotes the constant steady state power consumption of components like some sensors or communication devices. Depending on the components recruited for a CS, the corresponding instantaneous consumption may significantly change, as Eq. 1 denotes.

$$P(CS) = \sum_{i=1}^{n_1} \alpha_i \cdot P_{Dyn\ i} + \sum_{j=1}^{n_2} \beta_j \cdot P_{Stat\ j} \quad (1)$$

Where n_1 is the number of dynamic components, n_2 the number of static components, while α_i and β_j are 1 if the

Table 1 Control schemes and hardware components (○: optional, ●: required)

Control schemes	Software		Hardware			
	Control & Guidance	*Navigation*	*Sensors*			*Actuators*
			Sonars	*Lasers*	*Camera*	
FM	Forward Motion		○	○	○	●
SPF-OA	Path-following with obstacle avoidance	ODO	○	○-○	–	●
		QRCN	○	○-○	●	
		GBL	○	●-●		
CM-OA	Reactive centring control with obstacle avoidance	ODO	○	●-●	–	●
		QRCN	○	●-●	●	
RVT	Rotational visual tracking				●	●
IA	Image Analysis	–	–	–	●	–

The ○-○ symbol means that one of the two laser devices can be optionally chosen and the ●-● symbol means that the two laser devices are required

considered component is involved in the current CS and 0 otherwise.

The energy consumption of a CS (Eq. 2) conventionally obtained by multiplying the instantaneous power consumption by the active duration ΔT of a CS.

$$E(CS) = P(CS) \cdot \Delta T(CS) \tag{2}$$

Based on this formulation, for the robot battery, according to the hardware architecture and the selected control scheme $CS \in \{FM, SPF, CM, RVT, IA\}$ the following equation can be proposed:

$$\begin{aligned} P(CS) = {} & \alpha_1 P_{R_{Motion}}(v) + \alpha_2 \cdot P_{R_{US}}(f) \\ & + \beta_1 \cdot P_{R_{Kinect}} + k_1 \cdot \beta_2 \cdot P_{R_{Laser}} \end{aligned} \tag{3}$$

Where $k_1 \in \{0, 1, 2\}$ denotes the number of active lasers. α_i (dynamic) and β_i (static) are Boolean coefficients that indicate if the corresponding component is used or not.

For the laptop battery Eq. 1 can be developed in Eq. 4, for the considered platform, according to the selected control scheme CS and the external device connections EC (sensors, switchboards, Kinect).

$$\begin{aligned} P_L(CS) = {} & P_{L_{Proc}}(CS, EC) + P_{L_{Robot}} + P_{L_{Watt}} \\ & + \beta_1 \cdot P_{L_{Screen}} + \beta_2 \cdot P_{L_{Kinect}} + k_1 \cdot \beta_3 \cdot P_{L_{Laser}} \\ & + \beta_4 \cdot P_{L_{Switch_1}}(k_2) + \beta_5 \cdot P_{L_{Switch_2}}(k_3) \end{aligned} \tag{4}$$

Where:

β_1 to β_5 are Boolean coefficients representing the connection, or not, with corresponding external devices.

$k_1 \in \{1, 2\}$ represents the number of connected lasers.

$k_2 \in \{0, 1, 2\}$ represents the number of external devices connected with the processor via the switchboard 1. 0, 1 or 2 lasers can be connected.

$k_3 \in \{0, 1, 2\}$ denotes the number of external devices connected to the processor via the switchboard 2. 0 for no connection and 1 for the Kinect connection. 2 is still available for another connection.

So, the problem now is to identify independently each part of these models.

2.3 Instantaneous Power Consumption: The Proposed Process

To determine the instantaneous power consumption the followed process summarized in Fig. 2, can be decomposed into the following steps.

1. The process can be done for each separate supplying battery.
2. A detailed analysis of the hardware architecture allows to put in light the hardware components physically linked with a battery according to the different Control Schemes. Static components can be distinguished from the dynamic ones.

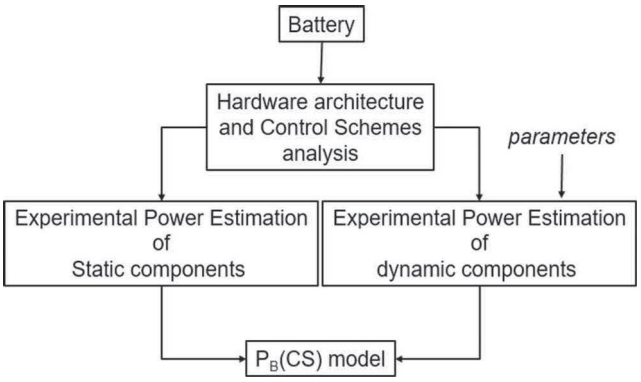

Fig. 2 Experimental process for power consumption identification

3. Depending on the component class, two different approaches must be used:
   - The constant consumption of the static components can be measured externally using adapted wattmeter/current/voltage measurement devices. For a robot the component consumption can also be measured directly in situ using an embedded wattmeter. For a laptop, if the access to the battery is not easy, the power consumption can be measured on-line using dedicated software functions of monitoring.
   - For the dynamic components the first work is to identify the relevant parameters influencing the power consumption using for example Ishikawa diagrams [10]. Sometimes a theoretical analysis can be engaged where acceptable simplifying assumptions must be adopted. Then these parameters must be tuned to determine the consumption behaviour using adapted experimental procedure.
4. Once the power consumption identification is completed, the generic formulation (Eqs. 3 and 4) of the battery power consumption P_B is obtained.

Finally, the last step is to estimate the accuracy of the proposed formulations.

2.4 Energy Models Evaluation: Experimental Context

To validate the proposed consumption models two types of experiments have been performed to estimate their accuracy.

On one hand we focused specifically on the accuracy of the energy consumption model of the forward motion using different sensors configurations and implementing or not a localization technique.

On the other hand we address more globally the accuracy of the proposed energy models along a 200 m long patrolling mission, implementing different control schemes and various robot velocities. In the laboratory corridors of

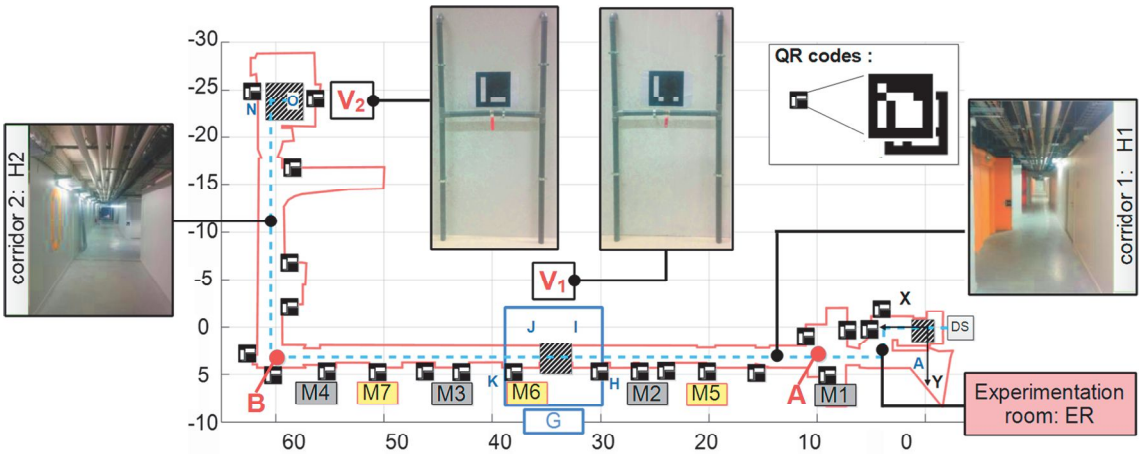

Fig. 3 The experimental context

Fig. 3 the mission is to monitor the the state (open or close) of 2 valves and to go back.

The global objectives and consumption identification of the proposed work being exposed, the next paragraph details and evaluates the obtained experimental consumption model of the robot and its on-board laptop.

3 Consumption Models and Evaluation

This paragraph presents the identification of the instantaneous power consumption of the static and dynamic components. When it is relevant or possible these results are compared with previous works. Finally the robot and laptop models are evaluated according to their accuracy.

3.1 Robot Battery

3.1.1 Static Components

Table 2 shows the measured power consumption of the static components, which remains constant as long as these sensors are activated.

The most energy-consuming sensor is the camera, with $P_{RKinect} = 2.82$ W. Each of the two laser sensors consumes $P_{RLaser} = 2.34$ W. Using both lasers requires 4.68 W. Finally, the measured consumption of the robot controller, electronic boards and embedded wattmeter when the robot is not moving $P_{R\_Controller1} = 2.67$ W.

Table 2 Power consumption of static components

Static component	Power (W)
Camera	$P_{RKinect} = 2.82$
Robot controller	$P_{R\_Controller1} = 2.67$
Hokuyo laser	$P_{RLaser} = 2.34$

3.1.2 Dynamic Components

Dynamic components are dissipative elements which can be parametrized at the CS level. We consider in the sequel the desired forward velocity v that plays an instrumental role in the motion energy profile, and the recruitment frequency, denoted f, for the sonar.

Firstly we address the motion energy consumption model that directly impacts the robot battery consumption.

DC motor actuators are dynamic components whose energy consumption depends on the acceleration and velocity control. The DC motor motion power model for Pioneer 3DX robots has been widely studied (Sadrpour, Tokekar, Mei, Kim, etc.). Hereafter we consider the DC power consumption model of Eq. 5 [1].

$$P_{R_{Motion}}(a, v) = C_1 \cdot a(t)^2 + C_2 \cdot v(t)^2 + C_3 \cdot v(t) + C_4 + C_5 \cdot a(t) + C_6 \cdot a(t) \cdot v(t) \quad (5)$$

Often in a robotic mission, the robot path can be divided into different parts where the velocities of the robot can be considered constant once the static regime is reached. Note that the tangential acceleration effects are negligible by the non-holonomic nature of the unicycle. Hence, robot acceleration becomes null, and from Eq. 5 only C_2, C_3 and C_4 parameters remain present. This constant velocity assumption is usually made at this point in the literature [2, 24, 25] and [21]. The consideration of system dynamics, as tackled in [14] and [28], results in complex and hard to manipulate models. Based on this assumption, the motion power model is simplified in Eq. 6.

$$P_{BR_{Motion}}(v) = C_2 \cdot v^2 + C_3 \cdot v + C_4 \quad (6)$$

From experimental measurements (Fig. 4), the analytic determination of parameters in Eq. 6 leads to:

$$C_2 = 6.25\ ;\ C_3 = 9.79\ ;\ C_4 = 3.66 \quad (7)$$

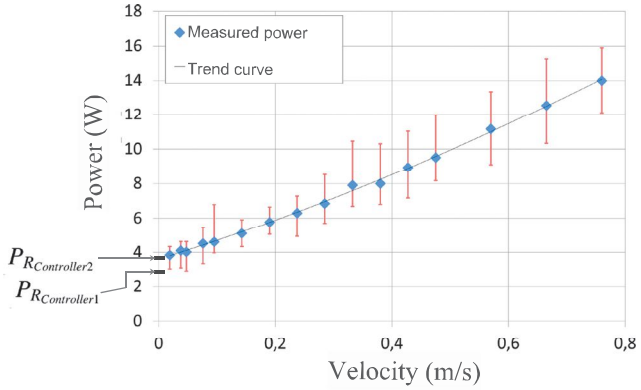

Fig. 4 DC motor motion power versus velocity. Straight forward movement with constant velocities are considered

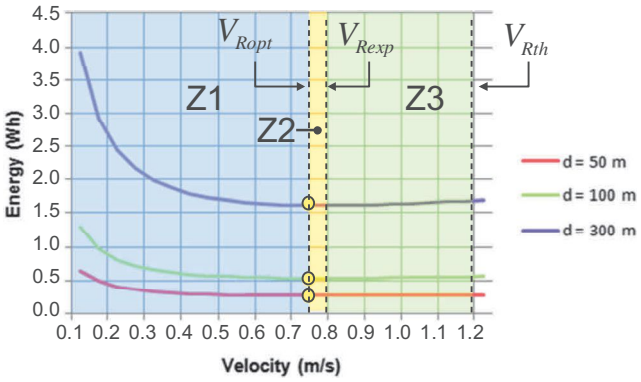

Fig. 5 Motion energy consumption for different distances

When the robot does not move, the power is C4 (3.66 W). This power $P_{R_{Controller2}}$ corresponds to the steady state consumption required by the different electronic boards, including the embedded wattmeter and the micro-controller within the robot. This constant consumption is removed from experimental data when the consumption model of other hardware components are under study.

Note that normally $P_{R_{Controller2}}$ would be equal to $P_{R_{Controller1}}$, but this is not the case. $P_{R_{Controller1}}$ is in fact obtained using extrapolation. While $P_{R_{Controller1}}$ is measured by applying motion control using $v = 0$ m/s. Integration of the experimental value $P_{R_{Controller1}}$ for the determination of Eq. 6 coefficients decreases the quality of the fit. We thus propose the following formulation to model the power consumption:

$$\begin{cases} P_{BR_{Motion}}(v) = P_{R_{Controller1}} = 2.67 & if\ v = 0 \\ P_{BR_{Motion}}(v) = 6.25 \cdot v^2 + 9.79 \cdot v + P_{R_{Controller2}} & \\ \qquad\qquad = 6.25 \cdot v^2 + 9.79 \cdot v + 3.66 & if\ v \neq 0 \end{cases} \quad (8)$$

Hereafter, the quadratic Eq. 6, which must be used when the robot is moving, will only be considered.

Moreover, from Eqs. 2 and 6, considering that $v = d/\Delta T$, where d denotes the travelled distance at constant velocity $v > 0$ during ΔT, the following energy motion modelling equation can apply for the motion energy consumption:

$$E_{R_{Motion}}(d, v) = C_2 \cdot d \cdot v + C_3 \cdot d + C_4 \cdot \frac{d}{v}. \quad (9)$$

This equation is very interesting and useful since it allows for estimating the motion energy needed to travel over a distance d at velocity v. Figure 5 represents, from Eq. 9, the theoretical motion energy required to travel a distance d at velocity v.

This new curve shows that even if the power consumption is weak for low velocities, the energy consumption needed to travel a given distance increases sharply for low velocities.

These energy curves show a minimum for an optimal velocity V_{Ropt}, which is expressed as:

$$\frac{\partial E_{R_{Motion}}(d, v)}{\partial v} \Rightarrow V_{Ropt} = \sqrt{\frac{3.66}{6.25}} = 0.76\ m/s \quad (10)$$

This optimal velocity induces minimum motion energy consumption E_{Ropt} for (V_{Ropt}). Three different areas can be distinguished from these curves.

- Z1 where $v < V_{Ropt}$
- Z2 where $V_{Ropt} < v \leqslant V_{Rexp}$. Note that the maximal velocity cannot be practically reached due to internal default limitation. This induces a significant decrease in the maximal attainable forward velocity of the robot, which is reduced experimentally from V_{Rth} = 1.2 m/s to V_{Rexp} = 0.75 m/s.
- Z3 where $V_{Rexp} < v \leqslant V_{Rth}$. This area can be studied theoretically but cannot be used experimentally for the used robot because of the previous limitation.

A generic formulation of optimal velocity considering the sensor impact is expressed in Eq. 11 using the generic power consumption expressed in Eq. 3, and with the same reasoning as that used previously to establish the optimal velocity.

$$V_{Ropt} = \sqrt{\frac{C_4 + \alpha_2 \cdot P_{R_{US}}(f) + \beta_1 \cdot P_{R\_Kinect} + k_1 \cdot \beta_2 \cdot P_{R_{Laser}}}{C_2}} \quad (11)$$

On the one hand, many works concerning power consumption modelling are based on electrical and mechanical laws. Kim in [14] conducted a very complete and detailed analysis of the energy consumption of a wheeled mobile robot like the Pioneer 3DX to determine the minimum-energy motion velocity profile, for straight line motion. A close reasoning is proposed in [27] and [28] to build energy optimal velocity profiles for robot DC motors. However, more complex motion paths are considered using a simplification of Eq. 5.

On the other hand, some studies used black box like models directly extracted from experimental measurements.

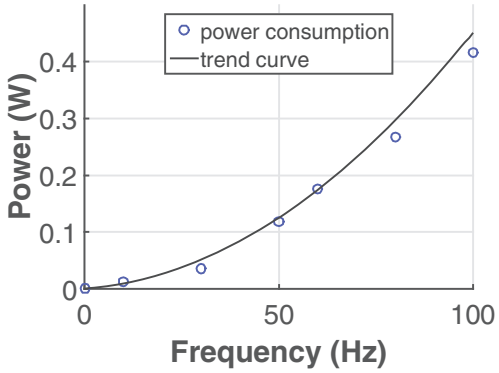

Fig. 6 Power consumption of one sonar cell

From the power versus angular velocity curve, the power behaviour is modelled using a second or sixth-degree polynomial equation whose coefficients are estimated from experimental curves. This approach is used in [31] to estimate the motion efficiency of different motion plans. Mei et al. in [31] used the second degree polynomial experimental model to deploy a set of mobile robots that cover an area under energy and time constraints. This work was referenced in Zhang et al. [32, 33] and was also used in Brateman et al. in [6] to model the power consumption of a Pioneer 3DX robot to investigate the energy minimization problem.

The model proposed in this work clearly belongs to the second class. However the generic formulation of the robot battery consumption explicitly integrates the impact of all the devices used. Moreover the formulation of Eq. 9 and its use for a given distance of straight movement seems to be original, putting in light the existence of a robot velocity minimizing energy consumption. So the proposed model is a good compromise between hard closed-form equation which are difficult to manipulate, and more simplistic global model not very accurate.

Secondly, the sonar sensor is another example of dynamic components because its energy consumption depends on the frequency rate. The sonar power consumption is experimentally identified and reported in Fig. 6 for different frequencies f.

A polynomial curve trend of Eq. 12 was built from experimental data.

$$P_{R_{US}}(f) = 4 \cdot 10^{-5} \cdot f^2 + 5.1 \cdot 10^{-4} \cdot f \tag{12}$$

Experimentally, the standard working frequency is 25 Hz, which corresponds to $P_{R_US}(25) = 0.037W$. The same study was carried out in [19], but was restricted to a linear approximation.

3.2 Laptop Battery

The energy provided by the laptop battery depends on three main factors: the laptop processor, internal components such as the hard drive and communication boards, external components like the screen and connection devices, such as USB.

The processor consumption P_{Proc} has been widely studied for CMOS-based chips. CPU power can also be de divided into dynamic and static parts. The Dynamic power consumption P_{Dyn} is dissipated when switching activity of the processor occurs. This power part can be approached by applying a cubic polynomial law of the CPU clock frequency when a low voltage level is used for the processor [7]. The Static power (or idle power) P_{Stat} corresponds to the power consumption when the processor has no tasks to execute. It is lower than the dynamic power but not negligible.

This processor power model was used in [32, 33] to control the processor frequency for recognition tasks using a Pioneer 3DX robot. The same model is used in [6] to control the frequency of the processor to reduce energy consumption while preventing robot collision.

This initial CPU processor model can be refined considering that the static part depends linearly on the processor frequency and adding DRAM or cache memory access consumption as a constant [15].

The laptop internal components also impact the energy consumption. However, these components, such as hard disks, network boards (typically 1W [23, 26], etc., consume almost constant power [5]. Their standard deviation between active and idle activities is generally considered to be small.

External device connection has an important impact on energy consumption. Two main sources can be considered. The screen display is a major source of consumption for a laptop, including blacklight [6]. The second is the USB connections with external components such as sensors (lasers, Kinect), switchboards or robot control processors. USB can provide power to low powered peripherals up to 2.25 W. Depending the type of peripheral, the current can reach 0.5 A [16] from the bus for USB 1.x and 2.0 and up to 0.9 A for USB 3.x. That corresponds to maximal power consumption ranging from 2.5 W to 4.5 W depending on the considered USB specification.

From this analysis, it is clear that the laptop battery must supply several internal and external components and devices. Moreover, depending on the hardware and software configuration needed for a CS, the corresponding CPU consumption can significantly change.

In the sequel, the laptop battery power consumption models are based on detailed analysis of the power consumption of the different external hardware devices, which are trigged by a given CS. The experimental results proposed are based on external experimental measurements combined with on-line monitoring of the battery current and voltage. Experimental power measures are periodically recorded over a time interval. In the following, the processor values correspond to the mean of the recorded values.

Table 3 Laptop power consumption of external laptop devices

External device	Power (W)		
Laser	0.400 (each)		
Robot controller	0.075		
Kinect	1.200		
Wattmeter	0.490		
Switch board	no relay activated	1 relay activated	2 relays activated
	0.087	0.405	0.720

3.2.1 Static/External Components

The static consumption of the laptop battery corresponds to the external links using USB connections. Although the robot battery externally supplies sensors, USB communication with the sensors and the switchboards with the laptop impact the laptop battery consumption. The measured power consumption, for the different configurations are summarized in Table 3.

3.2.2 Dynamic/Internal Components

The laptop integrates many internal energy-consuming devices. This internal consumption depends on many factors like the currently running processes, hard drive access, electric fan, wifi board consumption and of course the laptop processor. Unfortunately it is hard to differentiate the impacts of each factor. However, as supposed in [20] and [19], all of these factors can be integrated in a single power consumption factor P_{LProc} considered as constant for a given control scheme and external hardware configuration.

Table 4, summarizes the experimental data acquired considering the software and hardware elements involved in different control schemes. In this table, the control schemes, their hardware configurations, and their corresponding consumptions are presented horizontally. Vertically, this table can be divided into different parts : The control scheme, the involved sensors and actuators, the sensors, actuators, screen, processor consumption, the robot and laptop battery consumption and their corresponding percentages. The locomotion consumption impact was measured by considering a velocity of 0.1 m/s for RVT and 0.5 m/s for all other control schemes. All of the different control scheme configurations were implemented and tested but, for readability, in the sequel we present only an analysis focusing mainly on direct actuation control (FM).

The important screen power consumption is measured to $P_{LScreen}$ is 2.69 W, hence, it must be turned off during a mission.

3.3 Experimental Evaluation of Energy Consumption Models

3.4 Control Schemes Consumption : Global Analysis

By applying Eq. 3 for different sensor configurations, each control scheme leads to a very broad power consumption range, with regard to the robot battery consumption. If we focus on the Forward Motion control scheme in Table 4, depending on the chosen configuration, the power consumption can go from 10.12 W to 17.66 W for the 12 possible choices. The corresponding power consumption difference between the minimal and maximal values is 74.5%, thus highlighting the huge energy impact of the selected sensors on the battery consumption.

Overall, in this Table, if all of the proposed CS configurations are considered, the power consumption extracted from the robot battery can range from 4.7 W (SPF-OA/ODO control scheme with only the DC motor) up to 17.66 W when all sensors are mobilised. Note, moreover, that the energetic impact on the robot battery can be the same for different control schemes when the same sensors and actuators are involved. However, the laptop battery impact will differ because the algorithms used can differ.

Focussing now on the processor power consumption for different hardware configurations. Table 4 shows for example, for the Forward-Motion CS (FM) that the consumption ranged from 10.81 W to 13.34 W. Hence, depending on the sensor configuration (required by the algorithm use), the same CS power consumption of the laptop processor can differ up to 23%.

Considering all possible control schemes and hardware combinations, the processor power consumption ranged from 10.81 W (FM with one laser) up to 14.15 W (CM with sonars, two lasers and the Kinect).

More generally, the robot and laptop power consumptions have been combined to estimate the overall power needs. For the Forward Motion CS, the overall power needed for the robotic system ranges from 22.23 W to 34.68 W when the screen display is disconnected. The robot and laptop part are roughly identical. The maximal difference (9%) is observed for $P_R = 45.49\%$ and $P_L = 54.51\%$. This result is confirmed for all control schemes and configurations except for the IA and RVT control schemes. For these tasks, the laptop power consumption represents roughly 70% of the total power needed.

3.4.1 Trajectory Sensibility

In this part, different motion control schemes are used to move along the corridor H1 between the A and B points along 20 or 50 m (Fig. 10). As in many research studies, straight moving was chosen because most of the

Table 4 Detailed power consumption of the robotic system: Experimental data

			Sensors			Locomotion		Robot Battery	PC Battery												
			US	LAS	KIN	Stop	DC Motor (0.5 m/s)	DC Motor (0.1 m/s)	P_R (W)	$P_{L\ Kinect}$	$P_{L\ Laser}$	$P_{watt\ +Robot\ *}$	$P_{L\ Switch1}$	$P_{L\ Switch2}$	$P_{L\ screen\ **}$	$P_{L\ Proc}$	P_L (W)	$\%P_{Screen}$	$P_{Total} = P_R + P_L$	$\%P_R$	$\%P_L$	ΔP
RVT			0	0	1	0	0	1	7,52	1,20	0,00	0,57	0,09	0,41	2,69	13,38	15,64	14,68	23,16	32,47	67,53	35,06
SPF	*ODO*		0	0	0	0	1	0	4,70	0,00	0,00	0,57	0,09	0,09	2,69	11,00	11,74	18,65	16,44	28,60	71,40	42,81
			0	0	0	0	1	0	10,12	0,00	0,00	0,57	0,09	0,09	2,69	11,75	12,49	17,72	22,61	44,75	55,25	10,49
	QRCN		0	0	1	0	1	0	12,94	1,20	0,00	0,57	0,09	0,41	2,69	13,10	15,36	14,90	28,30	45,72	54,28	8,56
			1	1	1	0	1	0	15,32	1,20	0,40	0,57	0,41	0,41	2,69	13,72	16,69	13,88	32,01	47,85	52,15	4,29
			1	2	1	0	1	0	17,66	1,20	0,80	0,57	0,72	0,41	2,69	13,27	16,96	13,69	34,62	51,00	49,00	2,01
			0	1	1	0	1	0	15,28	1,20	0,40	0,57	0,41	0,41	2,69	13,66	16,63	13,92	31,91	47,88	52,12	4,24
			0	2	1	0	1	0	17,62	1,20	0,80	0,57	0,72	0,41	2,69	13,21	16,90	13,73	34,52	51,04	48,96	2,08
	GBL		0	2	0	0	1	0	14,80	0,00	0,80	0,57	0,72	0,09	2,69	13,90	16,37	16,43	31,17	47,48	52,52	5,04
FM			1	2	1	0	1	0	17,66	1,20	0,80	0,57	0,72	0,41	2,69	13,33	17,02	13,65	34,68	50,92	49,08	1,83
			0	2	1	0	1	0	17,62	1,20	0,80	0,57	0,72	0,41	2,69	13,27	16,96	13,69	34,58	50,95	49,05	1,90
			1	1	1	0	1	0	15,32	1,20	0,40	0,57	0,41	0,41	2,69	13,34	16,31	14,16	31,63	48,43	51,57	3,14
			0	1	1	0	1	0	15,28	1,20	0,40	0,57	0,41	0,41	2,69	13,28	16,25	14,20	31,53	48,46	51,54	3,08
			1	2	0	0	1	0	14,84	0,00	0,80	0,57	0,72	0,09	2,69	11,54	13,71	16,40	28,55	51,97	48,03	3,94
			0	2	0	0	1	0	14,80	0,00	0,80	0,57	0,72	0,09	2,69	11,48	13,65	16,46	28,45	52,02	47,98	4,04
			1	0	1	0	1	0	12,98	1,20	0,00	0,57	0,09	0,41	2,69	12,78	15,04	15,17	28,02	46,32	53,68	7,37
			0	0	1	0	1	0	12,94	1,20	0,00	0,57	0,09	0,41	2,69	12,72	14,98	15,22	27,92	46,34	53,66	7,31
			1	1	0	0	1	0	12,50	0,00	0,40	0,57	0,41	0,09	2,69	10,87	12,33	17,91	24,83	50,33	49,67	0,67
			0	1	0	0	1	0	12,46	0,00	0,40	0,57	0,41	0,09	2,69	10,81	12,27	17,98	24,73	50,38	49,62	0,76
			1	0	0	0	1	0	10,16	0,00	0,00	0,57	0,09	0,09	2,69	11,43	12,17	18,10	22,33	45,49	54,51	9,02
			0	0	0	0	1	0	10,12	0,00	0,00	0,57	0,09	0,09	2,69	11,37	12,11	18,18	22,23	45,52	54,48	8,96
IA			0	0	1	1	0	0	5,49	1,20	0,00	0,57	0,09	0,41	2,69	11,74	14,00	16,12	19,49	28,17	71,83	43,66
CM			1	2	1	0	1	0	17,66	1,20	0,80	0,57	0,72	0,41	2,69	14,15	17,84	13,10	35,50	49,74	50,26	0,52
			0	2	0	0	1	0	14,80	0,00	0,80	0,57	0,72	0,09	2,69	12,30	14,47	15,68	29,27	50,56	49,44	1,12
			1	2	0	0	1	0	14,84	0,00	0,80	0,57	0,72	0,09	2,69	12,36	14,53	15,62	29,37	50,52	49,48	1,04
			0	2	1	0	1	0	17,62	1,20	0,80	0,57	0,72	0,41	2,69	14,09	17,78	13,14	35,40	49,77	50,23	0,46

*Pwatt + robot : Basic consumption when system is stopped

*PL screen is measured but unused during mission (screen is off)

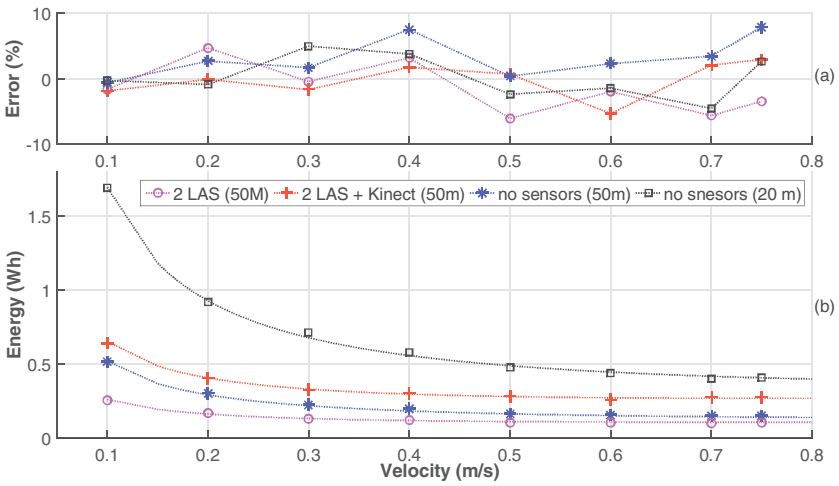

Fig. 7 **a** Model error **b** Experimental and theoretical robot energy consumption

time a robot mission involves straight lines with few rotations [14, 31].

Firstly we consider a simple Foward Motion without any global localization or obstacle avoidance. Figure 3 shows the robot battery energy measured, and the model error for different robot velocities for three external configurations: no sensors used, two lasers or two lasers and the Kinect connected. For energy, the represented points are experimental data. Curves show the theoretical prediction model with and without sensors.

The model error is ranged from -6% to +8% while the error mean ranged from -1.41% to +3.14%. The standard deviation was roughly constant at around 3%. As a first evaluation, there was a close fit between the theoretical curves and the experimental measurements (Fig. 7).

Q6

Concerning the laptop point of view the curves of Figure 8 are obtained. The theoretical curves and experimental measurements fit closely too. More precisely, the energy measurements fit the model prediction with an error ranging from -6.6% to 2.6%, and with a negative error mean of less than 2.8%. The standard deviation was approximately 2.5%.

These results demonstrate that theoretical laws accurately predict the power and energy consumption when forward motion is considered and different sensors are connected. However the experiment was done in open-loop. That is to say that the robot is supposed to follow the imposed path.

Now, focusing only on robot battery consumption we secondly consider that the control periodically adjusts the robot velocity and orientation to follow the defined 50 m long straight line path with a constant linear forward velocity. These experimentations show the impact of the closed-loop (control and localization methods) on the actual distance travelled and the robot velocity. These conditions differ from those used in Kim and Kim [14] and Tokekar et al. [28], where the robot was assumed to be permanently on the desired path.

In a first step the same previous experiment is redone with a closed loop control law based only on odometer information without any other sensors (dead reckoning).

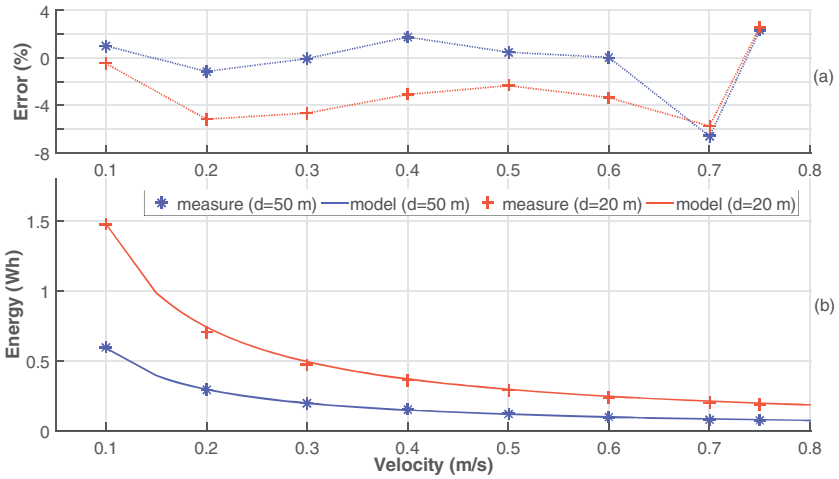

Fig. 8 **a** Model error **b** Experimental and theoretical laptop energy consumption

Table 5 Experimental results for different motion controls

	Velocity (m/s)	0.1	0.3	0.5
Energy	Predicted (Wh)	1.30	0.57	0.41
Simple Forward Motion	Experiment (Wh)	1.31	0.54	0.40
	Error (%)	0.53	4.34	0.95
Energy	Predicted (Wh)	1.30	0.57	0.41
Centring Motion	Experiment (Wh)	1.49	0.63	0.48
	Error (%)	12.55	12.99	14.36
Energy Exp. 1	Predicted (Wh)	1.69	0.67	0.48
QR-Code Motion	Experiment (Wh)	1.88	0.78	0.58
	Error (%)	10.10	14.10	17.24
Energy Exp. 2	Predicted (Wh)	1.69	0.67	0.48
QR-Code Motion	Experiment (Wh)	1.86	0.76	0.53
	Error (%)	9.13	11.84	9.43

Without global or local localization information, the robot is unaware of its odometric drift error. In a second step we implement a Centring Motion control using the lasers information. The irregularity of the environment generates a path adaptation inducing a trajectory that differs from the expected one. Finally the last experiment mixes dead reckoning with periodic QR-codes relocalization using less (Exp.1 (M1, M2, M3, M4)) or more markers (Exp.2 (M1 to M8)) of corridor H1 Fig. 3. Table 5 summarizes the main results of these different experiments. Values are rounded to the hundredth.

The simple open-loop Forward Motion Constrol Scheme shows a limited energy error less than 5% but the robot is not aware that it doesn't follow the desired path. Logically for the centring motion a higher error of more than 10% due to the irregular environment is observed. The QR-code oriented localization highlights the impact of the localization frequency on the predicted energy. With QR-codes roughly located every 6-7 m (Exp. 2), the energy estimation of around 10% remains acceptable.

The experiments showed of course that the energy prediction errors remains acceptable when the theoretical path corresponds to the one followed by the robot (Simple Path Following). Then, when the robot trajectory deviates from its nominal path (increased distance and time), obviously the prediction error increased (Centring Motion or QR-code Based Localization). In the following, the energy estimation is evaluated for different control schemes during a long-term mission.

3.4.2 Mission Level

In this section, a patrolling mission is considered in the experimental environment of Fig. 3. Starting from the docking station situated in the experimental room (ER), the robot must reach the location of two valves (V1 and V2) across corridors H1 and H2 to determine if the valves are open or closed. Then the robot must go back to the docking station. The path to follow is modelled as a sequence of straight lines. The control laws used ensure smooth

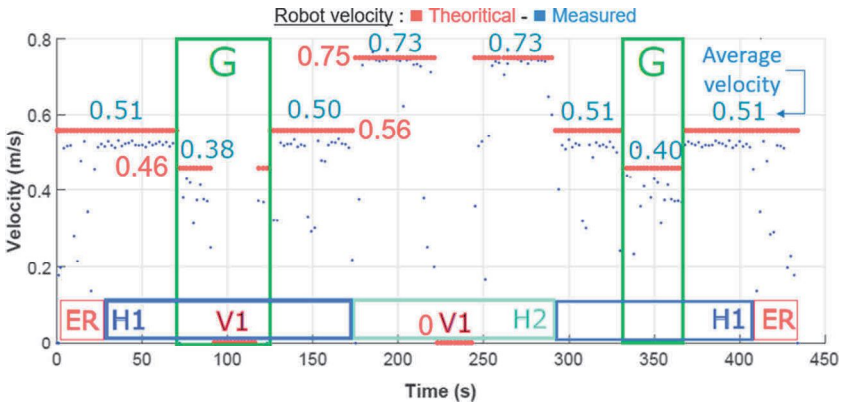

Fig. 9 Mission velocity experimental variations

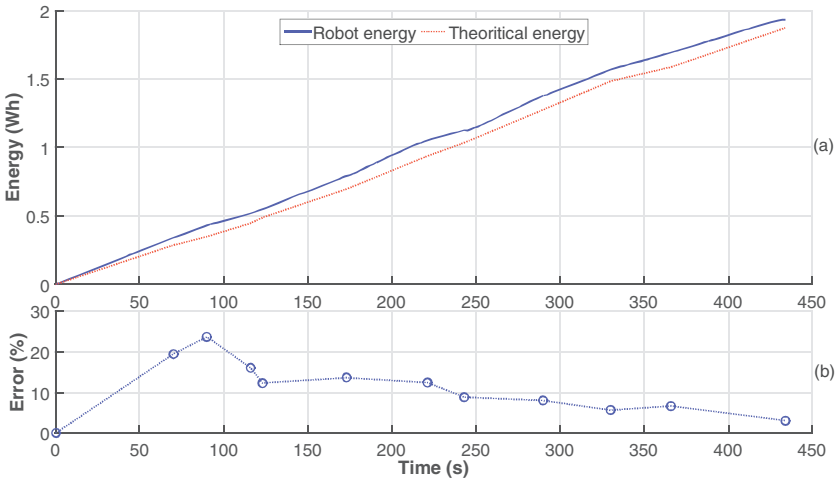

Fig. 10 **a** Mission experimental and theoretical robot energy consumption **b** Robot prediction error for the mission

path following and different control schemes are used to realized the mission. The mission is about 180 m long and takes around 7 minutes. To test the energy estimation accuracy, different velocities were imposed during the mission depending on the robot location: mainly 0.46 m/s, 0.56 m/s and 0.75 m/s. Figure 9 presents the theoretical (red line), measured (blue point) and average robot velocity during the proposed mission.

Differences between the expected and experimental values were due to the path following control, where the robot position was periodically corrected to accurately fit the expected path. In areas where many heading orientation changes were needed (turns in the experimental room and valve areas), the gap was around 10%. Due to these bends, the robot needs to move a quite long distance to stabilise its trajectory (no heading or velocity change). That explains the gap of 17.4% near V1 at the beginning of the mission (many heading orientation changes and short distance), and the 2.7% gap in corridor H2 (few heading orientation changes and long distance).

Figure 10a shows that the experimental robot energy consumption was slightly higher than expected. However, the curves are very similar. Moreover, the analysis illustrated in Fig. 10b demonstrates that the predicted energy estimation error after an initial peak with an error of 23.7% decreased to a final 10% error value. The initial peak was due to the nature of the initial part of the path when the robot turns a lot to come out the experimental room. For the rest of the mission, the difference between the expected path and the real path is small. Moreover, the energy consumption underestimation (maximal error) at the beginning of the mission gradually became negligible with regards to the overall energy consumption as the mission progressed. Considering the mission overall, the error mean was 11.5%, with a standard deviation of 6%.

The laptop (Fig. 11) and robot energy consumption curves are similar. The predicted energy was lower than the experimental energy. The behaviour error showed the same trend. The observed error was due to the difference between the real and expected trajectory, which increases

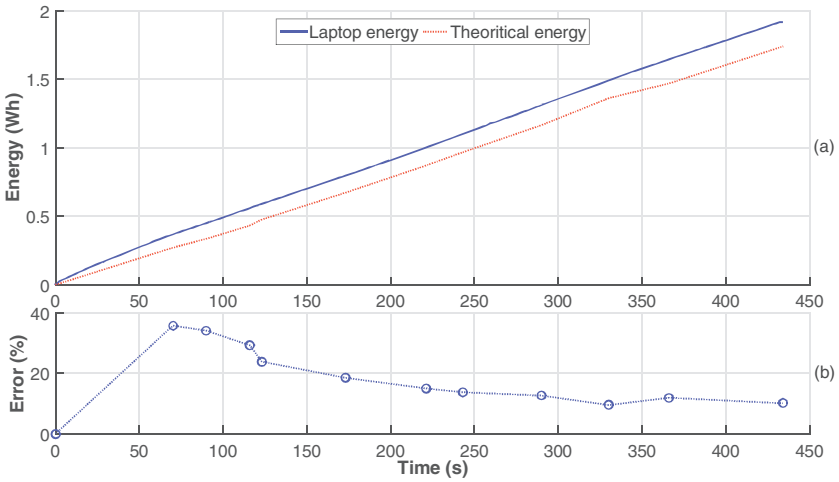

Fig. 11 **a** Mission experimental and theoretical laptop energy consumption **b** Laptop prediction error for the mission

the distance and duration necessary to cross the same linear distance. After an initial peak where the error was 35.9%, the energy consumption error decreased to 12.1% at the end of the mission. The mean error was 18.22%, with a standard deviation of 10.22%, for the overall mission.

These analyses demonstrated that the proposed power and energy consumption models allow a quite good estimation of the real consumption for missions with many different control schemes. The underestimation was due to the difference between the expected and real robot trajectory. When robot heading orientation changes were not frequent the consumption estimation was close to the real situation.

4 Conclusion and Future Researches

This paper presents a deep analysis of mobile robot system power and energy consumption. It focused on a Pioneer 3DX robot with an embedded laptop. This study investigated many issues that are seldom addressed in research studies on this topic.

The power and energy consumption of the robot and laptop were separately studied distinguishing static and dynamic components and considering different control schemes configurations. In the literature the robot battery is usually only considered, the laptop consumption was assumed to be constant or was not considered. The impact of a control scheme scheme configuration on energy consumption is also rarely addressed in the literature. Obviously the energy consumption clearly closely depends on the mobilized sensors and the chosen algorithms. So, these two sides of the issue must be considered in a long-term mission. This study also demonstrates that when the robot is moving along a straight line of known length with a constant velocity a simple closed-form relation links these parameters to the motion energy. Furthermore, to cross a given distance it exist a velocity minimizing the energy consumption. Finally experiments confirm the importance of accurate localization for efficient energy travelling and the good accuracy of the proposed consumption models along a patrolling mission. In conclusion, in a known environment, knowing the control schemes involved during a long-term mission, the models proposed in this study allow to predict the mission energy needs with an acceptable gap.

There were some obvious shortcomings in this study. The travelling power consumption model assumes, like many other studies, that mission can be divided into a set of straight lines where constant velocities can be applied. This hypothesis is often realistic when known environments are considered. But the acceleration impact would be integrated into power consumption models. However the proposed experiment showed that in spite of path following oscillations and several velocity changes, the power consumption model preserves acceptable accuracy. For robot field missions, it would be harder to meet the objectives due to environment variability. But like Sadrpour's approach [25] the robot power motion model could be enhanced by considering the impact of the road profile and the road surface conditions. The correlation between the robot location and power consumption should be also studied further in detail. Moreover, the consumption models are only usable considering a known path in a known environment. Finally, from an experimental view-point, the identification of the batteries power consumption needs an important experimental work. All control schemes with all possible sensors and actuators configurations must be experimentally studied.

Energy management is clearly a key issue for autonomous mobile robots [8]. The findings of this study could be useful for addressing many classes of robotic mission issues requiring a realistic estimation of robotic system energy consumption.

Energy oriented applications concerns for example energy-aware path planning problems as in [29]. However more accurate energy estimation models, like the ones we have proposed, must be implemented to enhance the accuracy of the proposed planning algorithms. So this work can help to increase the functioning time of robot systems between dockings.

It would be useful to manage energy consumption during long-term robotic missions in known environments. Depending on the available energy stock, the robotic task control and sensor configurations should be adapted throughout the mission to ensure that the mission can be completed. Using the proposed energy modelling we addressed this issue and proposed an approach where the robot can autonomously respect many mission performance objectives (Security, Energy, mission Duration) using dynamic software and hardware resources allocation [11] [12]. More recently in [17] the issue considering the links between localization and energy was also considered at the mission level.

Finally our on going studies concern underwater robotics and exploration missions. Based on this work, we build a global and complete energy consumption model for an underwater robot, whatever the motion followed and the sensors used. The final objectives is to use this energy model and our performance management approach to implement autonomous karstic exploration. Obviously our predictive energy model cannot be used for real exploration of underwater caves but it will be essential to decide when to stop the exploration part and to manage the way back to the meeting point. Q7

Author Contributions **Lotfi Jaiem**: Conceptualization, Methodology, Investigation, Writing - original draft. **Didier Crestani**: Conceptualization, Methodology, Data curation, Writing - review and editing. **Lionel Lapierre**: Conceptualization, Methodology, Investigation, review and editing. **Sebastien Druon**: Methodology and Software Validation.

Funding This project was supported by the LabEx NUMEV (ANR-10-LABX-0020) within the I-SITE MUSE (ANR-16-IDEX-0006) and the Region Occitanie (french FEDER funds).

Declarations

Competing interests The authors declare that they have no known competing financial interests or personal relationships that could have appeared to influence the work reported in this paper.

References

1. Dc motors, speed controls, servo systems. An engineering handbook Electro-Craft Corporation (1977)
2. Asikin, D., Dolan, J.M.: Reliability impact on planetary robotic missions. In: Intelligent Robots and Systems (IROS), 2010 IEEE/RSJ International Conference on, pp. 4095–4100. IEEE (2010)
3. Aylett, R.: Robots: bringing intelligent machines to life? a quarto book barron's (2002)
4. Benini, L., Bogliolo, A., De Micheli, G.: A survey of design techniques for system-level dynamic power management. IEEE Trans. VLSI Syst. **8**(3), 299–316 (2000). https://doi.org/10.1109/92.845896
5. Bircher, W.L., John, L.K.: Complete system power estimation using processor performance events. IEEE Trans. Comput. **61**(4), 563–577 (2012)
6. Brateman, J., Xian, C., Lu, Y.H.: Energy-efficient scheduling for autonomous mobile robots. IFIP VLSI-SoIC 2006 - IFIP WG 10.5, Int. Conf. VLSI Syst 361–366. https://doi.org/10.1109/VLSISOC.2006.313262 (2006)
7. Brooks, D.M., Bose, P., Schuster, S.E., Jacobson, H., Kudva, P.N., Buyuktosunoglu, A., Wellman, J., Zyuban, V., Gupta, M., Cook, P.W.: Power-aware microarchitecture: Design and modeling challenges for next-generation microprocessors. IEEE Micro **20**(6), 26–44 (2000)
8. Deshmukh, A., Vargas, P.A., Aylett, R., Brown, K.: Towards socially constrained power management for long-term operation of mobile robots (2011)
9. Ersal, T., Kim, Y., Broderick, J., Guo, T., Stefanopoulou, A., Siegel, J., Tilbury, D., Atkins, E., Peng, H., Jin, J., Ulsoy, A.: Keeping ground robots on the move through battery and mission management. ASME Dyn. Syst. Contr. Magaz. 1–6. https://doi.org/10.1115/6.2014-Jun-4 (2014)
10. Ishikawa, K., Lu, D.J.: What is total quality control ? : the Japanese way. Prentice-Hall Englewood Cliffs (1985)
11. Jaiem, L., Druon, S., Lapierre, L., Crestani, D.: A step toward mobile robots autonomy: Energy estimation models. 177–188 (2016)
12. Jaiem, L., Lapierre, L., Godary-Dejean, K., Crestani, D.: Toward performance guarantee for autonomous mobile robotic mission: An approach for hardware and software resources management. 189–195 (2016)
13. Kakogawa, A., Jeon, S., Ma, S.: Stiffness design of a resonance-based planar snake robot with parallel elastic actuators. IEEE Robot. Auto. Lett. 1–1. https://doi.org/10.1109/LRA.2018.2797261 (2018)
14. Kim, C.H., Kim, B.K.: Minimum-energy motion planning for differential-driven wheeled mobile robots. Inchopen 193–226 (2008)
15. Kim, M., Ju, Y., Chae, J., Park, M.: A simple model for estimating power consumption of a multicore server system. Int. J. Multimed. Ubiquitous Eng. **9**(2), 153–160 (2014)
16. Kollman, R., Betten, J.: Powering electronics from the usb port. Analog Applications Journal 29–35 (2002)
17. Lambert, P., Lapierre, L., Crestani, D.: An approach for fault tolerant and performance guarantee autonomous robotic mission. In: 13th NASA/ESA conference on adaptive hardware and systems, AHS 2019, pp. 87–94. https://doi.org/10.1109/AHS.2019.00009 (2019)
18. Lapierre, L., Zapata, R.: A guaranteed obstacle avoidance guidance system the safe maneuvering zone. Auton. Robot. **32**, 177–187 (2012). https://doi.org/10.1007/s10514-011-9269-5
19. Mei, Y.M.Y., Lu, Y.H.L.Y.H., Hu, Y., Lee, C.: A case study of mobile robot's energy consumption and conservation techniques. ICAR '05. In: Proceedings., 12th International Conference on Advanced Robotics 2005, pp 492–497. https://doi.org/10.1109/ICAR.2005.1507454 (2005)
20. Ogawa, K., Kim, H., Mizukawa, M., Ando, Y.: Development of the robot power management system adapting to tasks and environments-The design guideline of the power control system applied to the distributed control robot. In: 2006 SICE-ICASE International Joint Conference, pp 2042–2046. https://doi.org/10.1109/SICE.2006.315489 (2006)
21. Parasuraman, R., Pagala, P., Kershaw, K., Ferre, M.: Model based on-line energy prediction system for semi-autonomous mobile robots. In: 5th International conference on intelligent system modelling and simulation, pp 27–29 (2014)
22. Passama, R., Andreu, D.: ContrACT: a software environment for developing control architecture. In: CAR: Control Architectures of Robots. INRIA Grenoble Rhône-Alpes, Grenoble, France. https://hal.inria.fr/inria-00599683 (2011)
23. Sadrpour, A., Jin, J., Ulsoy, A.G.: Mission energy prediction for unmanned ground vehicles. In: Robotics and Automation (ICRA), 2012 IEEE International Conference on, pp. 2229–2234. IEEE (2012)
24. Sadrpour, A., Jin, J., Ulsoy, A.G.: Experimental validation of mission energy prediction model for unmanned ground vehicles. In: Proc. 2013 American Contrl Conference, pp 5980–5985 (2013)
25. Sadrpour, A., Jin, J.J., Ulsoy, A.G.: Mission energy prediction for unmanned ground vehicles using real-time measurements and prior knowledge. J. Field Robot. **30**(3), 399–414 (2013). https://doi.org/10.1002/rob.21453
26. Sohan, R., Rice, A.C., Moore, A.W., Mansley, K.: Characterizing 10 gbps network interface energy consumption. In: IEEE International conference on local computer networks, pp. 268–271 (2010)
27. Tokekar, P., Karnad, N., Isler, V.: Energy-optimal velocity profiles for car-like robots. In: Robotics and Automation (ICRA), 2011 IEEE International Conference on, pp. 1457–1462. IEEE (2011)
28. Tokekar, P., Karnad, N., Isler, V.: Energy-optimal trajectory planning for car-like robots. Auton. Robot. **37**(3), 279–300 (2014)
29. Wei, H., Wang, B., Wang, Y., Shao, Z., Chan, K.C.C.: Staying-alive path planning with energy optimization for mobile robots. Expert Syst. Appl. **39**(3), 3559–3571 (2012). https://doi.org/10.1016/j.eswa.2011.09.046
30. Xi, W., Remy, C.D.: Optimal gaits and motions for legged robots. In: 2014 IEEE/RSJ International conference on intelligent robots and systems, Chicago, IL, USA, September 14-18, 2014, pp. 3259–3265. IEEE. https://doi.org/10.1109/IROS.2014.6943015 (2014)
31. Mei, Y., Lu, Y.-H., Hu, Y.C., Lee, C.S.G.: In: IEEE International Conference on Robotics and Automation, 2004. Proceedings. ICRA '04. 2004, vol. 5, pp 4344–4349 (2004)
32. Zhang, W., Lu, Y.H., Hu, J.: Optimal solutions to a class of power management problems in mobile robots. Automatica **45**(4), 989–996 (2009). https://doi.org/10.1016/j.automatica.2008.11.004
33. Zhang, W.Z.W., Hu, J.H.J.: Low power management for autonomous mobile robots using optimal control. In: 2007 46th

IEEE Conference on Decision and Control, pp 5364–5369. https://doi.org/10.1109/CDC.2007.4434847 (2007)